NATIONAL AERONAUTICS AND SPACE ADMINISTRATION

INTERNAL NOTE NO. MSC-ES-R-69-2

DOCKING CAPTURE BOUNDARIES FOR APOLLO MISSIONS D, F, AND G

DISTRIBUTION AND REFERENCING

This paper is not suitable for general distribution or referencing. It may be referenced only in other working correspondence and documents by participating organizations.

MANNED SPACECRAFT CENTER
HOUSTON, TEXAS
July 29, 1969

INTERNAL NOTE MSC-ES-R-69-2

DOCKING CAPTURE BOUNDARIES FOR APOLLO MISSIONS D, F, AND G

PREPARED BY

David A. Hamilton
David A. Hamilton

John A. Schliesing
John A. Schliesing

APPROVED BY

John W. Kiker
John W. Kiker
Head, Landing and Docking Mechanics Branch

Joseph N. Kotanchik
Joseph N. Kotanchik
Chief, Structure and Mechanics Division

NATIONAL AERONAUTICS AND SPACE ADMINISTRATION
MANNED SPACECRAFT CENTER
HOUSTON, TEXAS
July 29, 1969

CONTENTS

TABLES

FIGURES

DOCKING CAPTURE BOUNDARIES FOR APOLLO MISSIONS D, F, AND G

By David A. Hamilton and
John A. Schliesing

SUMMARY

A digital computer simulation of the docking dynamics of both transposition and lunar orbit docking has been developed by the Landing and Docking Analysis Section. The simulation was used to investigate the docking capture performance for Apollo missions D, F, and G. Several primary contact parameters were designated and varied in order to consider a broad range of initial contact conditions. The parameters which were varied in the simulation included probe-drogue contact position, contact velocities, angular misalinements, and angular rates. These parameters were varied within the Apollo design value limits.

Results of the simulations provided the docking capture capability for the three missions. The capture capability for mission D was better in most cases than for missions F and G. In all missions, optimum capture performance occurred for transposition docking with the command and service module thrusting at probe-drogue contact and for lunar orbit docking with the lunar module thrusting at probe-drogue contact.

INTRODUCTION

The success of the Apollo missions is highly dependent on achieving a satisfactory spacecraft-to-spacecraft dock during the transposition and lunar orbit phases of the mission. Therefore, it is essential that docking capture capability be established prior to each mission. A digital computer simulation of the docking dynamics was developed to establish the capture capabilities.

The digital computer simulation uses a detailed mathematical model of the Apollo probe/drogue docking mechanism to determine load-time histories generated at the docking interface, and numerically integrates the six differential equations of motion of both the active and passive vehicles. The simulation accounts for the control system operation of

each vehicle throughout the docking dynamics. In reference 1, the simulation is described in more detail and a comparison of the experimental and computer-simulated results is given.

The capture capability was established for missions D, F, and G using the aforementioned computer analysis. A summation of the capture performance for the three missions is presented in this report.

SYSTEM CHARACTERISTICS

Mass Properties

The vehicle mass characteristics used in the digital simulations of the docking dynamics were taken from reference 2 for missions D and G and lunar orbit docking (LOD) of mission F. The transposition docking (TLD) mass properties of mission F were taken from a Marshall Space Flight Center memo.[1] Tables I and II show the mass properties which were used in the digital simulations of the three missions for TLD and LOD, respectively. Comparison of TLD mass properties for missions F and G shows that they are approximately the same, while comparison of LOD for missions D, F, and G shows that the properties of mission F are bracketed by those of missions D and G.

Probe-Drogue Characteristics

Nominal probe-drogue physical and geometric characteristics were used in the docking analysis.[2] The temperature condition of the probe drogue was assumed to be -20° F. This temperature assumption was used to establish conservative docking boundaries. The probe cylinder bending friction was highest at this low temperature; thus, the work efficiency of the probe was decreased with respect to its ambient temperature performance.

Contact Conditions

Initial probe-drogue contact conditions, which were varied in this study, included contact position, contact velocity, attitude misalinement,

---

[1]Memo R-P&VE-VAW-68-91 (MSFC). Subject: Saturn V/AS-505 Preliminary Predicted Operational Mass Characteristics, Depletion Cut-off.

[2]NAR Internal Letter to R. F. Nicholas from K. A. Bloom, Nov. 15, 1968. Subject: Docking System Characteristics.

and attitude rates. The impact point on the drogue surface was varied to achieve radial velocity impacts which were normal to the drogue surface (case 1), at ±45° to the drogue surface (case 2), and tangential to the drogue surface (case 3). The axial and radial velocities of the center of gravity of the active vehicle were varied to consider a wide range of contact velocities. Attitude misalinements and rates were varied to consider both nominal and extreme conditions. The radial miss distance, which is the distance measured radially outward from the drogue center line to the center of the ball joint supporting the probe tip, was varied to the extreme value of 1 foot.

Control Systems

For all the studies discussed in this paper, the command and service module (CSM) was placed in a spacecraft control system (SCS) narrow dead band attitude hold mode (0.2 degree dead band); the lunar module/Saturn IVB (LM/S-IVB) was placed in an SCS attitude hold mode (1.0 degree dead band); and the LM was placed in an SCS attitude hold mode (0.3 degree dead band). The results of these studies are also representative of docking in which the digital auto pilot (DAP) control system is used, since the docking disturbances are large and the resulting control torque of both the SCS and DAP systems are identical.

CAPTURE PERFORMANCE RESULTS

To define the capture performance of the Apollo docking mechanism for a given docking configuration, it is necessary to establish the allowable range of initial contact parameters, such as contact velocities, attitude misalinements, attitude rates, and radial miss distance. The primary contact parameters and their Apollo design values are given in figure 1. The pictorial definition of the primary contact parameters in figure 1 is shown in planar form, but the parameters have three-dimensional interpretations.

Transposition Docking

Simulations of transposition docking were made in two primary modes. Mode 1 was with the CSM thrusting at probe-drogue contact and maintaining the thrust until capture latch. Mode 2 was with neither vehicle thrusting. For all three missions, the mode 1 capture performance was significantly better than for mode 2. The TLD performance for mission D was better in both modes than for missions F and G. (Capture performance for missions F and G was considered the same in TLD because of their

similar mass characteristics; thus, actual digital simulations were not made for mission F.) Tables III to VIII and figures 2 to 7 present capture results for missions D and G in TLD. Tables III to VIII show capture times for various lateral velocity, axial velocity, angular misalinement, and angular rate combinations for mode 1. Figures 2 and 3, in which the axial and lateral velocities are varied, present the poorest mission D capture performance times for modes 1 and 2. Similar plots for mission G are presented in figures 4 and 5. Figures 6 and 7 show capture performance for axial velocity versus radial miss distance for mode 2 of missions D and G.

Lunar Orbit Docking

Simulations of lunar orbit docking were made in three primary modes. Modes 1 and 2 were with the CSM and LM, respectively, thrusting at probe-drogue contact and maintaining the thrust until capture latch. Mode 3 was with neither vehicle thrusting. Mode 1 performance for mission D was significantly better than for mission G. (Mission G LOD capture performance can be considered conservative performance for mission F because of mass characteristics; therefore, actual digital simulations of mission F were not made.) Mode 2 performance for both missions D and G, and also for mission F, was very good. Mode 3 performance was very poor for all three missions with the poorest performance being on mission G. Tables IX to XX and figures 8 to 12 present capture times for various lateral velocity, axial velocity, angular misalinement, and angular rate combinations for modes 1 and 2. Figures 8, 9, and 10, in which the axial and lateral velocities are varied, present the poorest capture performance times for modes 1 and 2. Figures 11 and 12 show capture performance of axial velocity versus radial miss distance for mode 3.

CONCLUDING REMARKS

The docking capture performance was established for missions D, F, and G using a digital program which simulated the docking dynamics. Results indicated that optimum capture performance in all missions for transposition docking was for the condition of the command and service module thrusting from initial probe-drogue contact until capture latch, and for lunar orbit docking was for the condition of the lunar module thrusting from initial probe-drogue contact until capture latch.

REFERENCES

1. Anon.: Correlation of Digital Simulations of Apollo Post-Contact Docking Dynamics. MSC Internal Note IN-67-ES-2, Jan. 1967.

2. Anon.: CSM/LM Spacecraft Operational Data Book. Vol. III, Mass Properties, Revision I, Nov. 1968.

TABLE I.- MASS CHARACTERISTICS FOR TRANSPOSITION DOCKING FOR MISSIONS D, F, AND G

Parameter	CSM			LM/S-IVB		
	D	F	G	D	F	G
Mass, slugs	1839.3	1976.5	1971.8	6906.	2058.	2077.
Moments of inertia, slugs-ft^2						
I_{xx}	31693.	34211.	34005.	106749.	101000.	102921.
I_{yy}	83106.	76475.	79058.	2330465.	1055000.	1064186.
I_{zz}	78721.	79193.	76183.	2332993.	1054000.	1064141.
Products of inertia, slugs-ft^2						
I_{xy}	520.1	--	92.	--	--	--
I_{xz}	-1955.4	--	-1829.	--	--	--
I_{yz}	-2891.6	--	-3210.	--	--	--
Center-of-gravity offset, ft						
Y	0.500	0.533	0.542	0.051	0.163	0.163
Z	-.310	-.333	-.333	-.094	-.241	-.258

TABLE II.- MASS CHARACTERISTICS FOR LUNAR ORBIT DOCKING FOR MISSIONS D, F, AND G

Parameter	CSM			LM ascent stage		
	D	F	G	D	F	G
Mass, slugs	840.6	1140.7	1140.1	303.3	247.0	176.8
Moments of inertia, slugs-ft^2						
I_{xx}	15360.	20881.	20227.	5894.	4723.	3300.
I_{yy}	52258.	63675.	63180.	3640.	3564.	2749.
I_{zz}	50784.	56986.	56604.	5844.	3853.	2303.
Products of inertia, slugs-ft^2						
I_{xy}	--	--	-861.	--	--	-31.
I_{xz}	--	--	-2041.	--	--	145.
I_{yz}	--	--	-374.	--	--	-392.
Center-of-gravity offset, ft						
Y	0.592	0.458	0.458	-0.200	-0.267	-0.333
Z	-.250	-.250	-.242	.175	.142	.183

TABLE III.- MISSION D TRANSPOSITION DOCKING

WITH CSM THRUSTING (CASE 1)

Radial velocity V_R, fps	Axial velocity V_A, fps	Capture time, sec	
		θ = 0 deg $\dot{\theta}$ = 0 deg/sec	θ = 10 deg $\dot{\theta}$ = 1 deg/sec
0.00	1.00	0.61	0.64
.25	1.00	.64	.97
.25	.75	1.10	1.22
.25	.50	1.47	1.51
.25	.25	2.05	1.89
.50	1.00	.90	1.06
.50	.75	1.19	1.34
.50	.50	5.55	1.77
.50	.25	6.35	2.49

TABLE IV.- MISSION D TRANSPOSITION DOCKING

WITH CSM THRUSTING (CASE 2)

Radial velocity V_R, fps	Axial velocity V_A, fps	Capture time, sec		
		θ = 0 deg $\dot{\theta}$ = 0 deg/sec	θ = 10 deg $\dot{\theta}$ = 1 deg/sec	θ = -10 deg $\dot{\theta}$ = -1 deg/sec
0.00	1.00	0.63	0.88	--
.25	1.00	.86	.98	--
.25	.75	1.17	1.25	--
.25	.50	5.18	1.57	--
.25	.25	2.40	2.15	--
.50	1.00	7.16	1.06	--
.50	.75	6.90	1.33	--
.50	.50	7.20	1.84	--
.50	.25	7.40	2.60	--
-.25	1.00	.60	--	0.64
-.25	.75	.81	--	.86
-.25	.50	1.20	--	1.22
-.25	.25	6.72	--	2.12
-.50	1.00	8.87	--	.63
-.50	.75	7.96	--	.85
-.50	.50	(X)	--	⟨X⟩
-.50	.25	icc	--	⟨X⟩

Note: (X) is greater than 10-second capture time, ⟨X⟩ is capture failure (jackknife condition), and icc is impossible contact condition.

TABLE V.- MISSION D TRANSPOSITION DOCKING

WITH CSM THRUSTING (CASE 3)

Radial velocity V_R, fps	Axial velocity V_A, fps	Capture time, sec	
		θ = 0 deg $\dot{\theta}$ = 0 deg/sec	θ = 10 deg $\dot{\theta}$ = 1 deg/ sec
0.00	1.00	0.63	0.93
.25	1.00	.84	.94
.25	.75	1.13	1.14
.25	.50	6.95	1.45
.25	.25	7.40	2.08
.50	.100	9.42	.78
.50	.75	9.20	1.13
.50	.50	7.22	⟨X⟩
.50	.25	7.40	⟨X⟩

Note: ⟨X⟩ is capture failure (jackknife condition).

TABLE VI.- MISSION G TRANSPOSITION DOCKING

WITH CSM THRUSTING (CASE 1)

Radial velocity V_R, fps	Axial velocity V_A, fps	Capture time, sec		
		θ = 0 deg $\dot{\theta}$ = 0 deg/sec	θ = 10 deg $\dot{\theta}$ = 1 deg/sec	θ = 10 deg $\dot{\theta}$ = -1 deg/sec
0.00	1.00	0.68	0.93	1.19
.25	1.00	1.00	.95	7.28
.25	.75	6.36	1.30	6.63
.25	.50	5.96	1.63	9.90
.25	.25	2.46	2.01	9.53
.50	1.00	6.25	1.50	7.29
.50	.75	6.48	⟨X⟩	8.13
.50	.50	ⓧ	⟨X⟩	⟨X⟩
.50	.25	9.86	2.77	⟨X⟩

Note: ⟨X⟩ is capture failure (jackknife condition), ⓧ is greater than 10-second capture time.

TABLE VII.- MISSION G TRANSPOSITION DOCKING

WITH CSM THRUSTING (CASE 2)

Radial velocity V_R, fps	Axial velocity V_A, fps	Capture time, sec		
		θ = 0 deg $\dot{\theta}$ = 0 deg/sec	θ = 10 deg $\dot{\theta}$ = 1 deg/sec	θ = -10 deg $\dot{\theta}$ = -1 deg/sec
0.00	1.00	0.87	1.08	0.78
.25	1.00	7.10	1.16	--
.25	.75	6.58	1.47	--
.25	.50	6.34	1.75	--
.25	.25	6.68	2.31	--
.50	1.00	(X)	⟨X⟩	--
.50	.75	(X)	⟨X⟩	--
.50	.50	6.47	⟨X⟩	--
.50	.25	8.29	3.00	--
-.25	1.00	.64	--	.74
-.25	.75	1.02	--	.95
-.25	.50	1.33	--	1.18
-.25	.25	7.42	--	6.29
-.50	1.00	9.61	--	.71
-.50	.75	(X)	--	.96
-.50	.50	9.62	--	(X)
-.50	.25	icc	--	(X)

Note: (X) is greater than 10-second capture time, ⟨X⟩ is capture failure (jackknife condition), and icc is impossible contact condition.

TABLE VIII.- MISSION G TRANSPOSITION DOCKING

WITH CSM THRUSTING (CASE 3)

Radial velocity V_R, fps	Axial velocity V_A, fps	Capture time, sec		
		θ = 0 deg $\dot{\theta}$ = 0 deg/sec	θ = 10 deg $\dot{\theta}$ = 1 deg/sec	θ = 10 deg $\dot{\theta}$ = -1 deg/sec
0.00	1.00	0.86	8.70	0.91
.25	1.00	8.17	1.06	(X)
.25	.75	6.60	6.51	(X)
.25	.50	9.68	5.42	7.86
.25	.25	6.76	2.28	7.55
.50	1.00	(X)	1.02	⟨X⟩
.50	.75	(X)	⟨X⟩	⟨X⟩
.50	.50	9.00	⟨X⟩	9.03
.50	.25	9.13	⟨X⟩	⟨X⟩

Note: (X) is greater than 10-second capture time, and ⟨X⟩ is capture failure (jackknife condition).

TABLE IX.- MISSION D LUNAR ORBIT DOCKING

WITH LM THRUSTING (CASE 1)

Radial velocity V_R, fps	Axial velocity V_A, fps	Capture time, sec	
		θ = 0 deg $\dot{\theta}$ = 0 deg/sec	θ = 10 deg $\dot{\theta}$ = 1 deg/sec
0.00	1.00	0.74	0.68
.25	1.00	.84	.78
.25	.75	1.08	.94
.25	.50	1.40	1.20
.25	.25	1.88	1.56
.50	1.00	.98	.91
.50	.75	1.32	1.10
.50	.50	1.73	1.44
.50	.25	2.10	1.92

TABLE X.- MISSION D LUNAR ORBIT DOCKING

WITH LM THRUSTING (CASE 2)

Radial velocity V_R, fps	Axial velocity V_A, fps	Capture time, sec		
		θ = 0 deg $\dot{\theta}$ = 0 deg/sec	θ = 10 deg $\dot{\theta}$ = 1 deg/sec	θ = -10 deg $\dot{\theta}$ = -1 deg/sec
0.00	1.00	0.72	0.72	0.78
.25	1.00	.84	.75	--
.25	.75	1.14	.97	--
.25	.50	2.09	1.24	--
.25	.25	2.83	1.65	--
.50	1.00	1.16	.89	--
.50	.75	1.47	1.18	--
.50	.50	2.84	2.08	--
.50	.25	3.82	3.39	--
-.25	1.00	.69	--	.72
-.25	.75	.91	--	1.65
-.25	.50	2.30	--	2.47
-.25	.25	2.27	--	2.66
-.50	1.00	2.35	--	1.65
-.50	.75	2.96	--	4.47
-.50	.50	2.59	--	2.95
-.50	.25	icc	--	3.36

Note: icc is impossible contact condition.

TABLE XI.- MISSION D LUNAR ORBIT DOCKING

WITH LM THRUSTING (CASE 3)

Radial velocity V_R, fps	Axial velocity V_A, fps	Capture time, sec	
		θ = 0 deg $\dot{\theta}$ = 0 deg/sec	θ = 10 deg $\dot{\theta}$ = 1 deg/sec
0.00	1.00	0.73	0.74
.25	1.00	.82	.76
.25	.75	1.92	1.80
.25	.50	2.47	2.28
.25	.25	3.08	2.93
.50	1.00	1.73	1.89
.50	.75	2.52	2.40
.50	.50	3.26	3.51
.50	.25	4.43	3.28

TABLE XII.- MISSION D LUNAR ORBIT DOCKING

WITH CSM THRUSTING (CASE 1)

Radial velocity V_R, fps	Axial velocity V_A, fps	Capture time, sec	
		θ = 0 deg $\dot{\theta}$ = 0 deg/sec	θ = 10 deg $\dot{\theta}$ = 1 deg/sec
0.00	1.00	0.84	0.74
.25	1.00	1.14	1.20
.25	.75	1.23	1.25
.25	.50	1.62	1.32
.25	.25	2.28	1.79
.50	1.00	2.74	1.71
.50	.75	1.51	1.70
.50	.50	2.05	1.69
.50	.25	2.56	2.29

TABLE XIII.- MISSION D LUNAR ORBIT DOCKING

WITH CSM THRUSTING (CASE 2)

Radial velocity V_R, fps	Axial velocity V_A, fps	Capture time, sec		
		θ = 0 deg $\dot{\theta}$ = 0 deg/sec	θ = 10 deg $\dot{\theta}$ = 1 deg/sec	θ = -10 deg $\dot{\theta}$ = -1 deg/sec
0.00	1.00	0.85	2.62	0.96
.25	1.00	2.43	1.31	--
.25	.75	3.30	1.17	--
.25	.50	3.40	1.53	--
.25	.25	4.26	2.06	--
.50	1.00	3.52	2.70	--
.50	.75	4.49	3.36	--
.50	.50	4.18	3.96	--
.50	.25	5.24	4.71	--
-.25	1.00	3.07	--	.85
-.25	.75	3.54	--	3.60
-.25	.50	4.10	--	3.93
-.25	.25	4.53	--	4.21
-.50	1.00	5.41	--	6.05
-.50	.75	6.43	--	6.26
-.50	.50	7.02	--	7.06
-.50	.25	icc	--	8.31

Note: icc is impossible contact condition.

TABLE XIV.- MISSION D LUNAR ORBIT DOCKING

WITH CSM THRUSTING (CASE 3)

Radial velocity V_R, fps	Axial velocity V_A, fps	Capture time, sec	
		θ = 0 deg $\dot{\theta}$ = 0 deg/sec	θ = 10 deg $\dot{\theta}$ = 1 deg/sec
0.00	1.00	0.82	2.23
.25	1.00	2.71	.92
.25	.75	3.53	1.18
.25	.50	3.53	3.03
.25	.25	4.90	3.88
.50	1.00	3.59	3.62
.50	.75	5.62	4.05
.50	.50	7.33	6.37
.50	.25	6.23	5.63

TABLE XV.- MISSION G LUNAR ORBIT DOCKING

WITH LM THRUSTING (CASE 1)

Radial velocity V_R, fps	Axial velocity V_A, fps	Capture time, sec		
		θ = 0 deg $\dot{\theta}$ = 0 deg/sec	θ = 10 deg $\dot{\theta}$ = 1 deg/sec	θ = 10 deg $\dot{\theta}$ = -1 deg/sec
0.00	1.00	0.69	0.63	0.78
.25	1.00	.79	.72	.90
.25	.75	.96	.84	1.03
.25	.50	1.14	1.00	1.24
.25	.25	1.40	1.21	1.40
.50	1.00	.90	.83	1.05
.50	.75	1.12	.97	1.21
.50	.50	1.30	1.16	1.39
.50	.25	1.48	1.41	1.50

TABLE XVI.- MISSION G LUNAR ORBIT DOCKING

WITH LM THRUSTING (CASE 2)

Radial velocity V_R, fps	Axial velocity V_A, fps	Capture time, sec		
		θ = 0 deg $\dot{\theta}$ = 0 deg/sec	θ = 10 deg $\dot{\theta}$ = 1 deg/sec	θ = -10 deg $\dot{\theta}$ = -1 deg/sec
0.00	1.00	0.70	0.69	0.75
.25	1.00	.80	.72	--
.25	.75	.99	.85	--
.25	.50	1.22	1.03	--
.25	.25	2.21	1.24	--
.50	1.00	2.29	.83	--
.50	.75	2.60	1.01	--
.50	.50	2.93	1.22	--
.50	.25	2.92	2.53	--
.25	1.00	.67	--	.70
.25	.75	.82	--	.89
.25	.50	1.95	--	1.71
.25	..25	1.93	--	1.95
.50	1.00	1.74	--	1.96
.50	.75	1.84	--	1.98
.50	.50	2.05	--	2.16
.50	.25	icc	--	2.60

Note: icc is impossible contact condition.

TABLE XVII.- MISSION G LUNAR ORBIT DOCKING WITH LM THRUSTING (CASE 3)

Radial velocity V_R, fps	Axial velocity V_A, fps	Capture time, sec		
		θ = 0 deg, $\dot{\theta}$ = 0 deg/sec	θ = 10 deg, $\dot{\theta}$ = 1 deg/sec	θ = 10 deg, $\dot{\theta}$ = -1 deg/sec
0.00	1.00	0.71	0.72	0.72
.25	1.00	1.65	.73	1.86
.25	.75	1.78	.87	2.69
.25	.50	2.08	1.85	2.89
.25	.25	2.31	2.77	2.88
.50	1.00	2.10	1.90	3.12
.50	.75	3.13	3.10	2.51
.50	.50	2.63	3.29	2.66
.50	.25	2.95	3.33	3.71

TABLE XVIII.- MISSION G LUNAR ORBIT DOCKING

WITH CSM THRUSTING (CASE 1)

Radial velocity V_R, fps	Axial velocity V_A, fps	Capture time, sec		
		θ = 0 deg $\dot{\theta}$ = 0 deg/sec	θ = 10 deg $\dot{\theta}$ = 1 deg/sec	θ = 10 deg $\dot{\theta}$ = -1 deg/sec
0.00	1.00	2.97	2.98	4.41
.25	1.00	3.70	3.17	3.37
.25	.75	3.69	3.69	3.85
.25	.50	2.04	1.51	4.18
.25	.25	2.96	2.14	2.61
.50	1.00	4.78	4.31	5.01
.50	.75	5.23	4.07	3.70
.50	.50	2.52	2.06	4.49
.50	.25	3.51	2.85	2.98

TABLE XIX.- MISSION G LUNAR ORBIT DOCKING

WITH CSM THRUSTING (CASE 2)

Radial velocity V_R, fps	Axial velocity V_A, fps	Capture time, sec		
		θ = 0 deg $\dot{\theta}$ = 0 deg/sec	θ = 10 deg $\dot{\theta}$ = 1 deg/sec	θ = -10 deg $\dot{\theta}$ = -1 deg/sec
0.00	1.00	2.85	5.19	4.15
.25	1.00	3.58	4.23	--
.25	.75	3.75	5.51	--
.25	.50	5.05	1.66	--
.25	.25	5.86	2.31	--
.50	1.00	4.06	4.09	--
.50	.75	4.91	4.65	--
.50	.50	8.16	5.62	--
.50	.25	Ⓧ	6.70	--
.25	1.00	6.11	--	4.53
.25	.75	6.45	--	6.45
.25	.50	5.10	--	4.74
.25	.25	6.04	--	6.71
.50	1.00	Ⓧ	--	Ⓧ
.50	.75	Ⓧ	--	Ⓧ
.50	.50	6.49	--	Ⓧ
.50	.25	icc	--	8.61

Note: Ⓧ is greater than 10-second capture time, and icc is impossible contact condition.

TABLE XX.- MISSION G LUNAR ORBIT DOCKING

WITH CSM THRUSTING (CASE 3)

Radial velocity V_R, fps	Axial velocity V_A, fps	Capture time, sec		
		θ = 0 deg $\dot{\theta}$ = 0 deg/sec	θ = 10 deg $\dot{\theta}$ = 1 deg/sec	θ = 10 deg $\dot{\theta}$ = -1 deg/sec
0.00	1.00	2.65	6.19	4.43
.25	1.00	4.30	4.80	6.82
.25	.75	4.37	4.25	8.06
.25	.50	5.07	3.94	8.03
.25	.25	8.28	6.62	6.61
.50	1.00	6.34	4.84	Ⓧ
.50	.75	6.40	Ⓧ	Ⓧ
.50	.50	8.79	Ⓧ	Ⓧ
.50	.25	Ⓧ	Ⓧ	Ⓧ

Note: Ⓧ is greater than 10-second capture time.

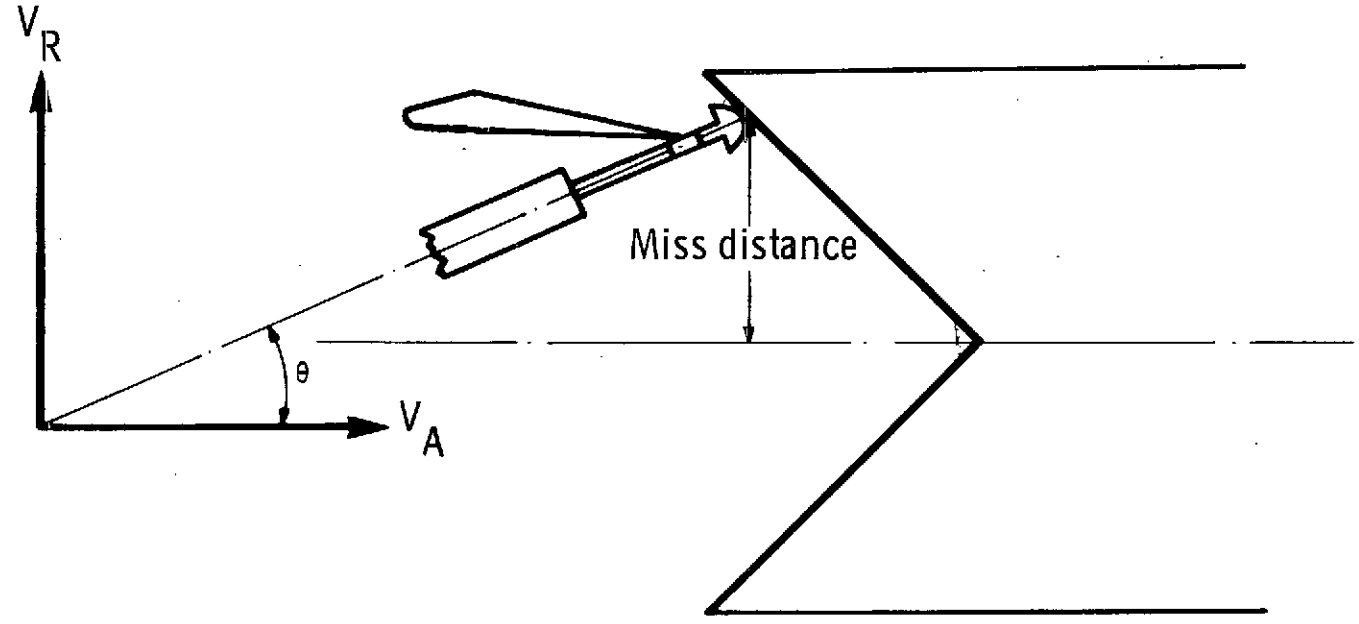

INITIAL CONTACT PARAMETERS

Axial closing velocity V_A, fps	0.1 - 1
Radial velocity V_R, fps	±0.5
Angular misalinement θ, deg	±10
Angular rate $\dot{\theta}$, deg/sec	±1
Miss distance, in.	±12

Figure 1.- Apollo docking criteria for initial contact parameters.

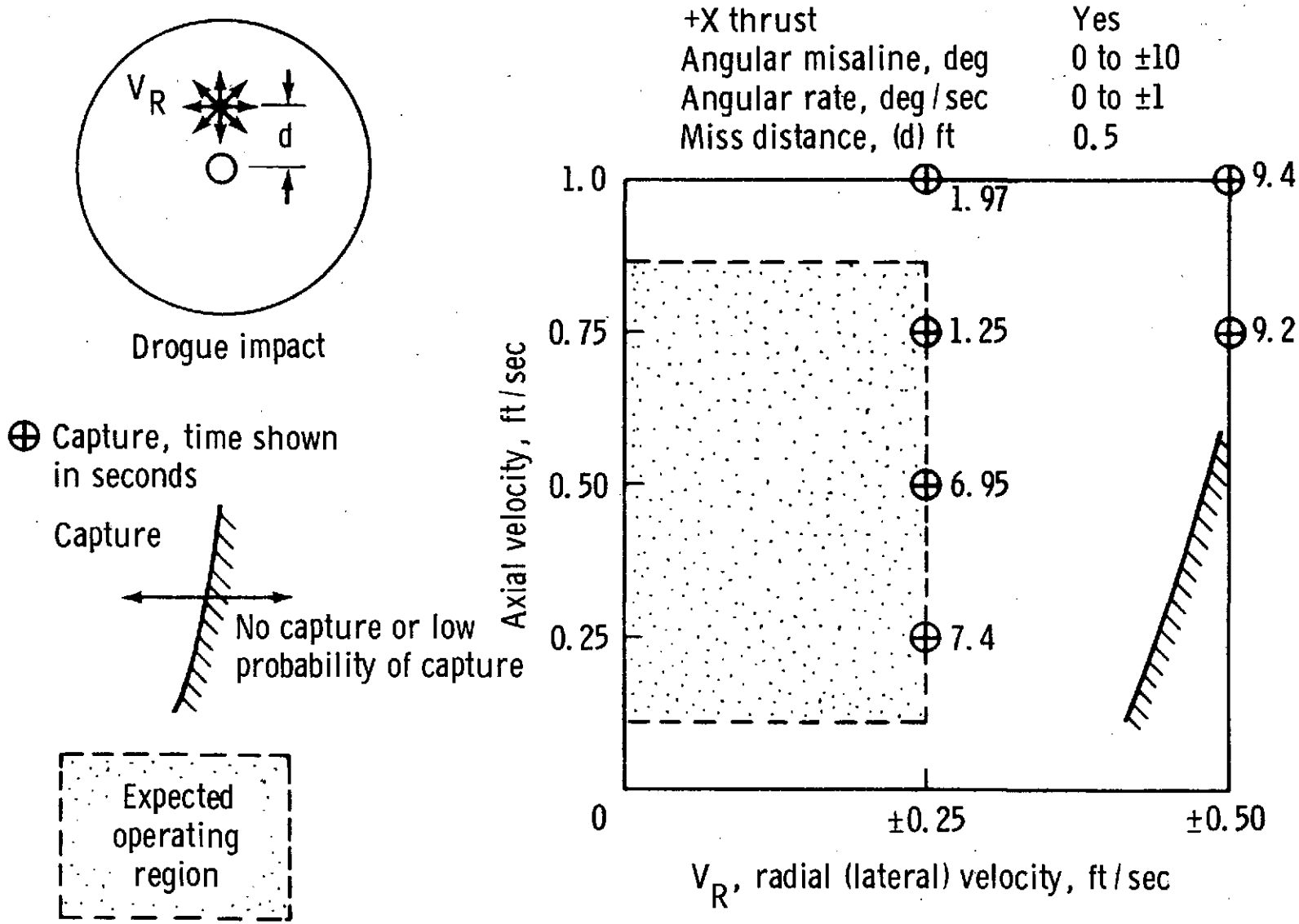

Figure 2.- Mission D, TLD capture boundaries for axial versus radial velocity with CSM thrust.

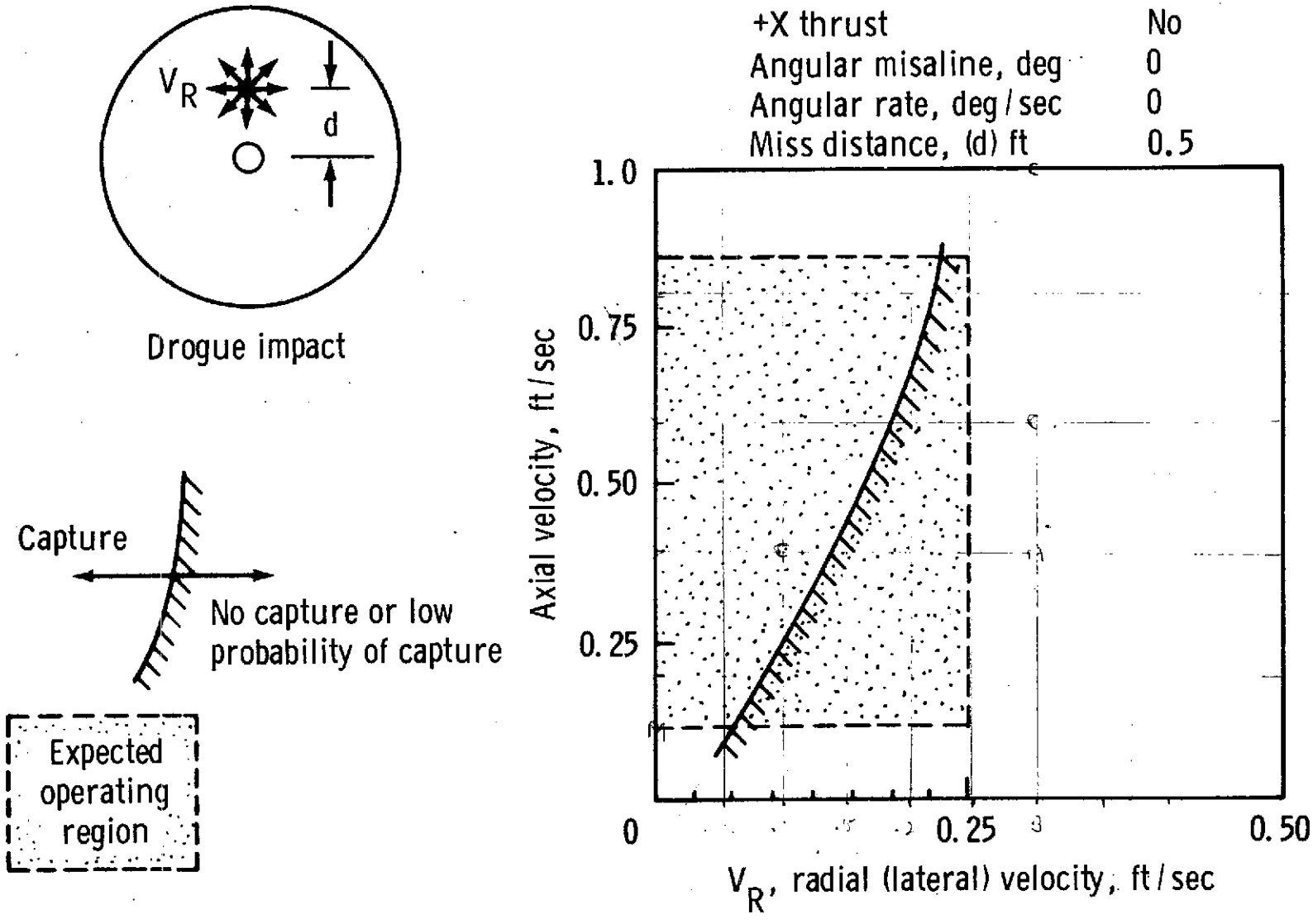

Figure 3.- Mission D, TLD capture boundaries for axial versus radial velocity with no thrust.

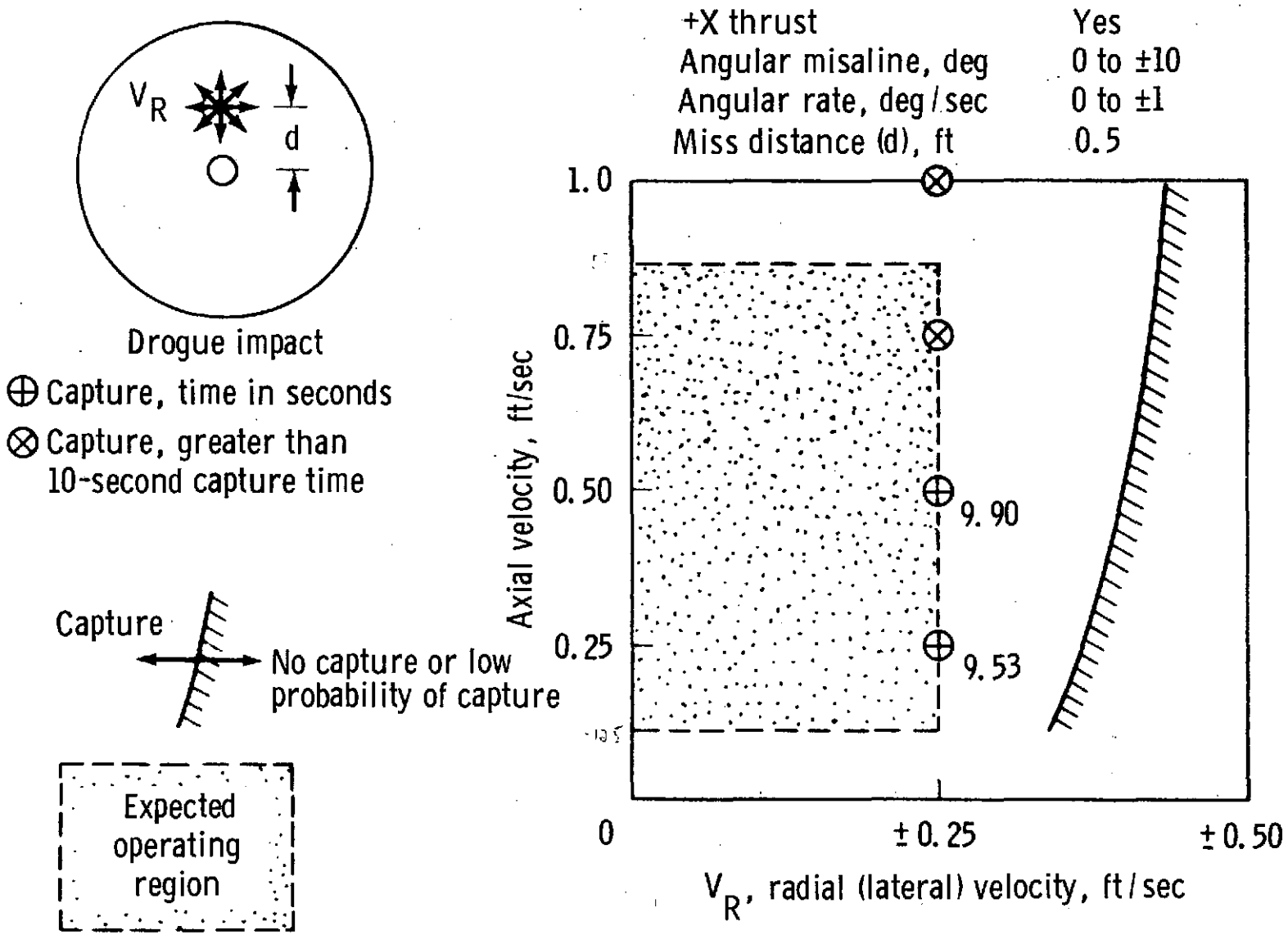

Figure 4.- Mission G, TLD capture boundaries for axial versus radial velocity with CSM thrust.

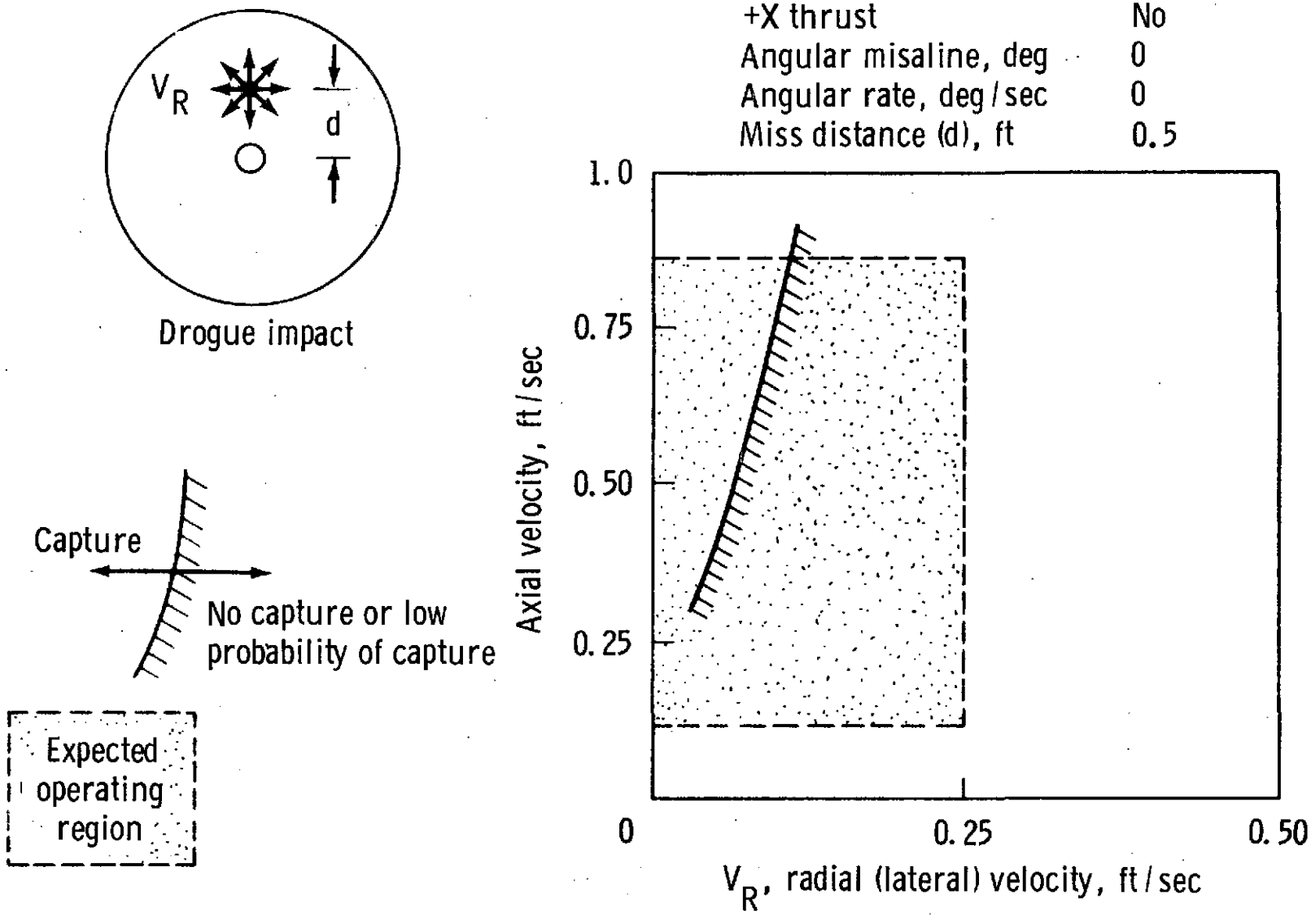

Figure 5.- Mission G, TLD capture boundaries for axial versus radial velocity with no thrust.

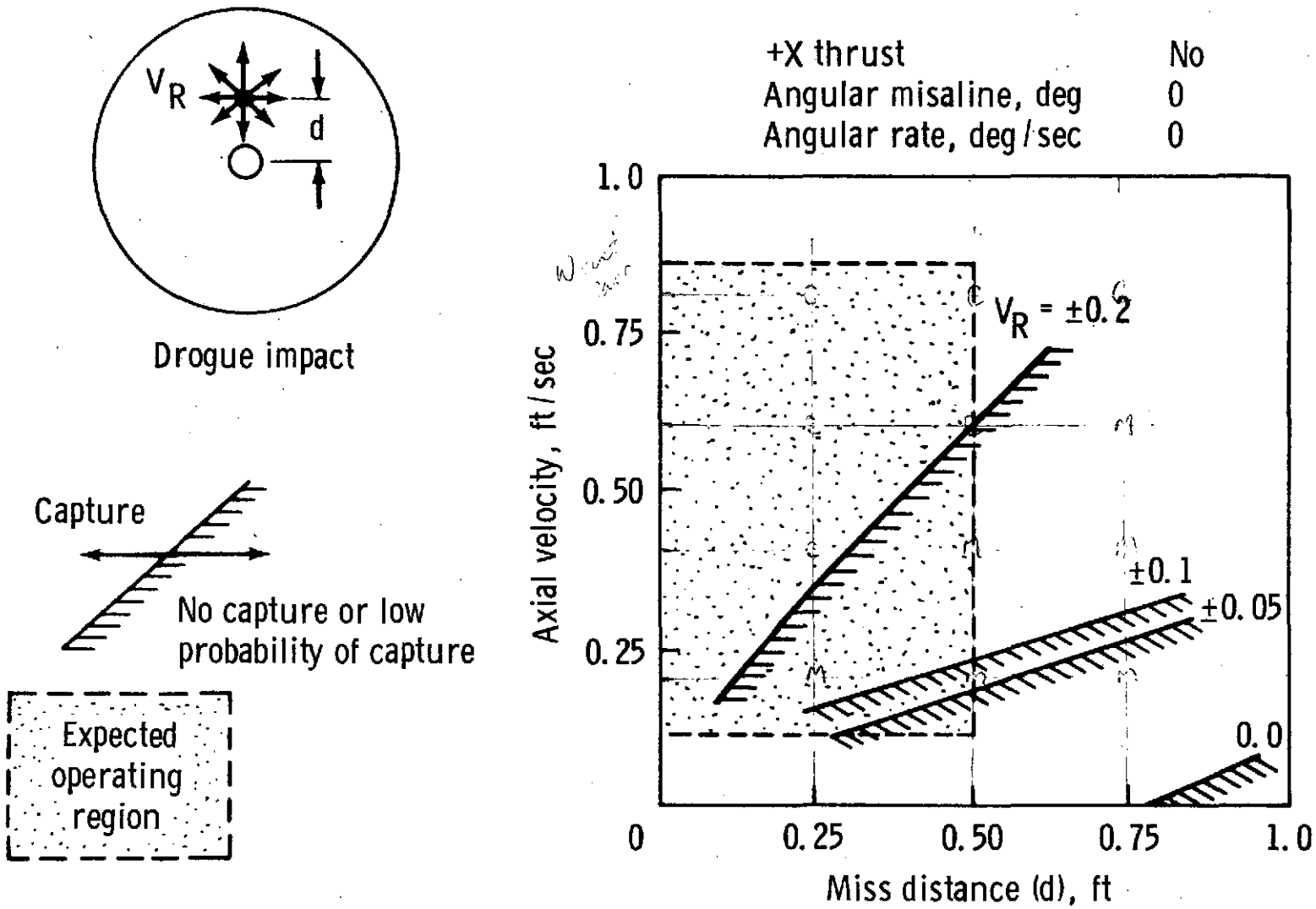

Figure 6.- Mission D, TLD capture boundaries for axial velocity versus radial miss distance with no thrust.

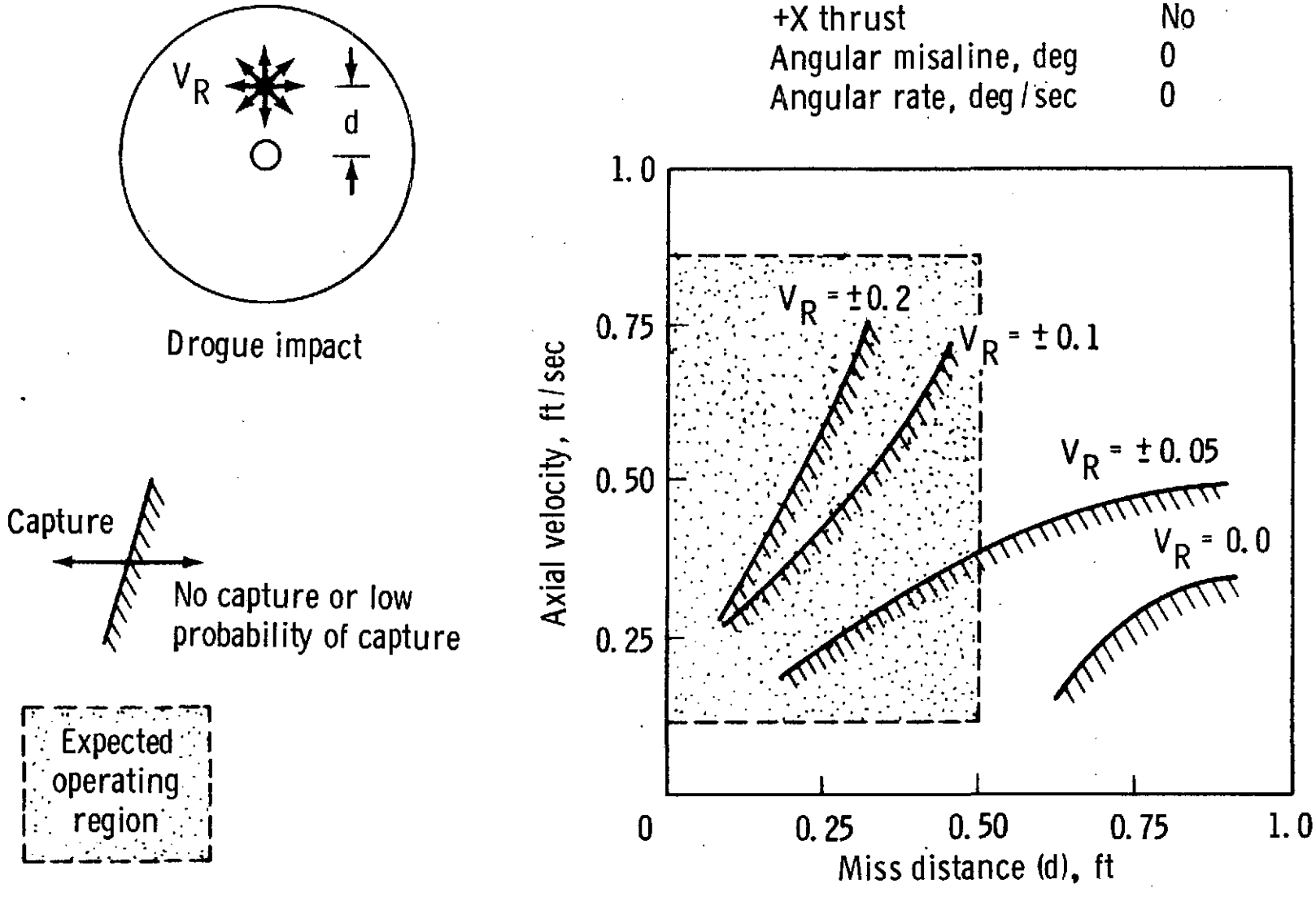

Figure 7.- Mission G, TLD capture boundaries for axial velocity versus radial miss distance with no thrust.

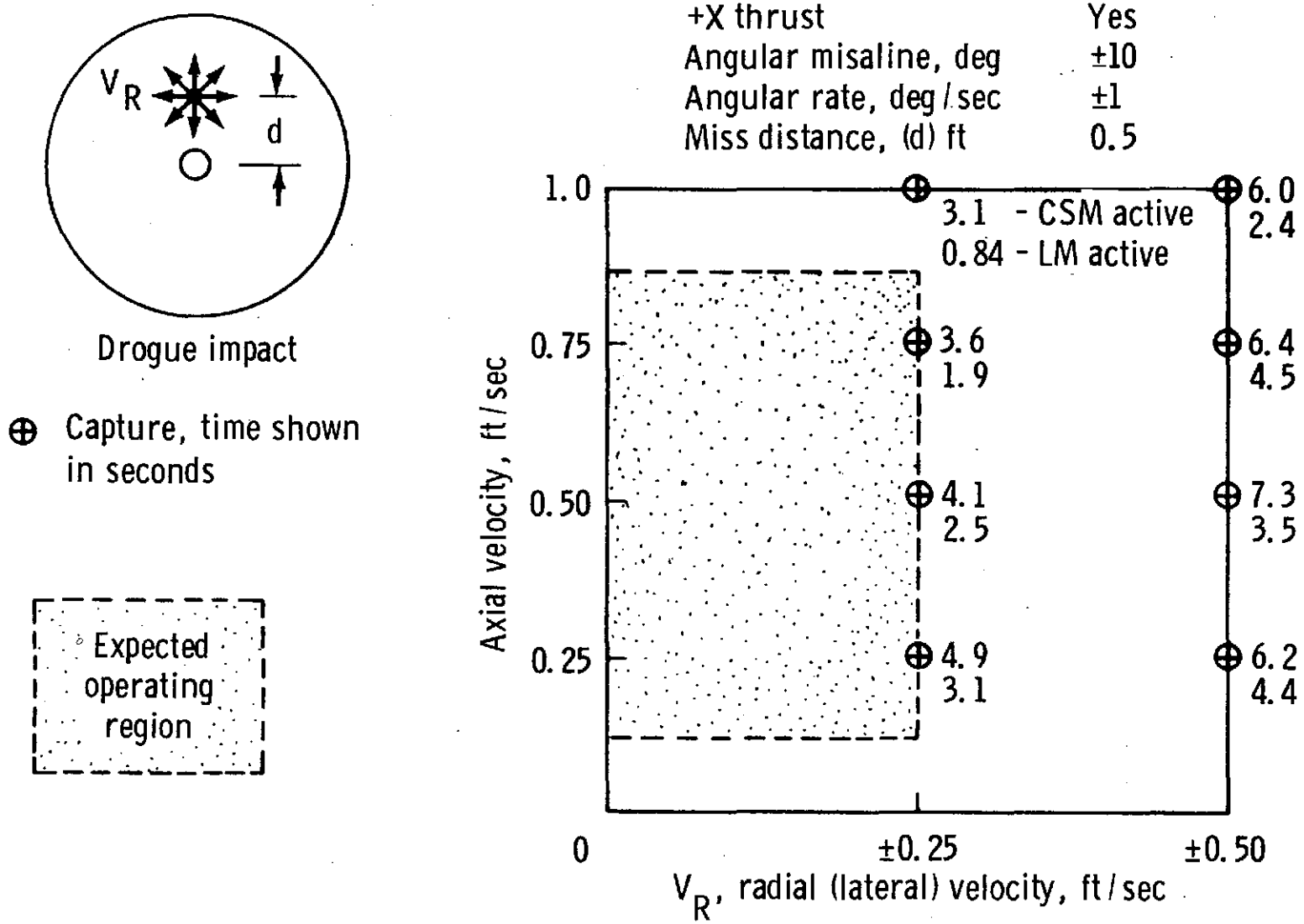

Figure 8.- Mission D, LOD capture boundaries for axial versus radial velocity with CSM or LM thrust.

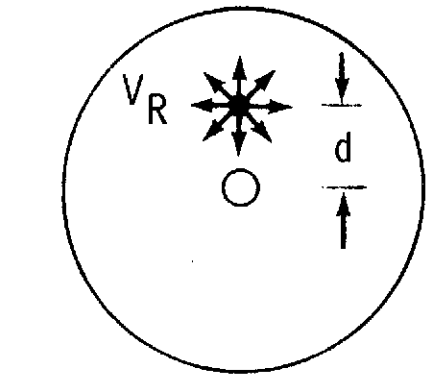

Drogue impact

⊕ Capture, time in seconds

Expected operating region

+X thrust (LM)	Yes
Angular misaline, deg	0 to +10
Angular rate, deg/sec	0 to +1
Miss distance (d), ft	0.5

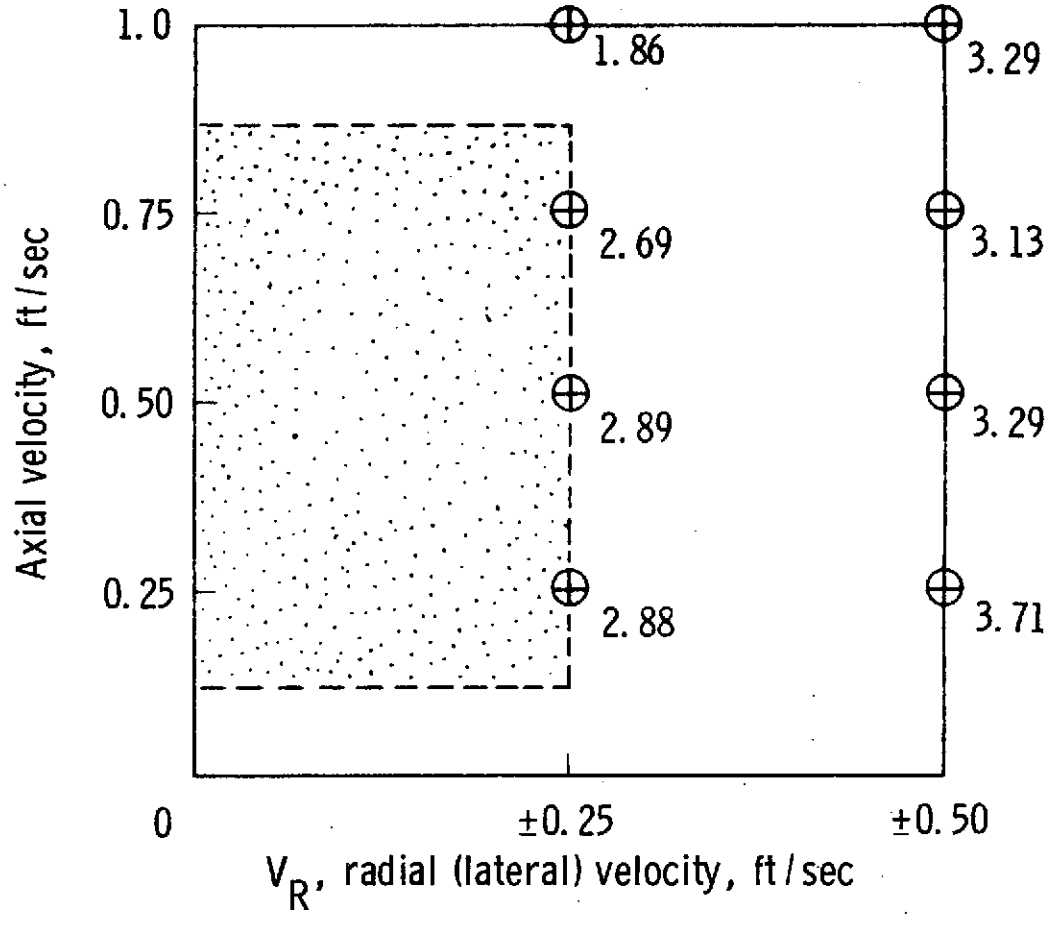

Figure 9.- Mission G, LOD capture boundaries for axial versus radial velocity with LM thrust.

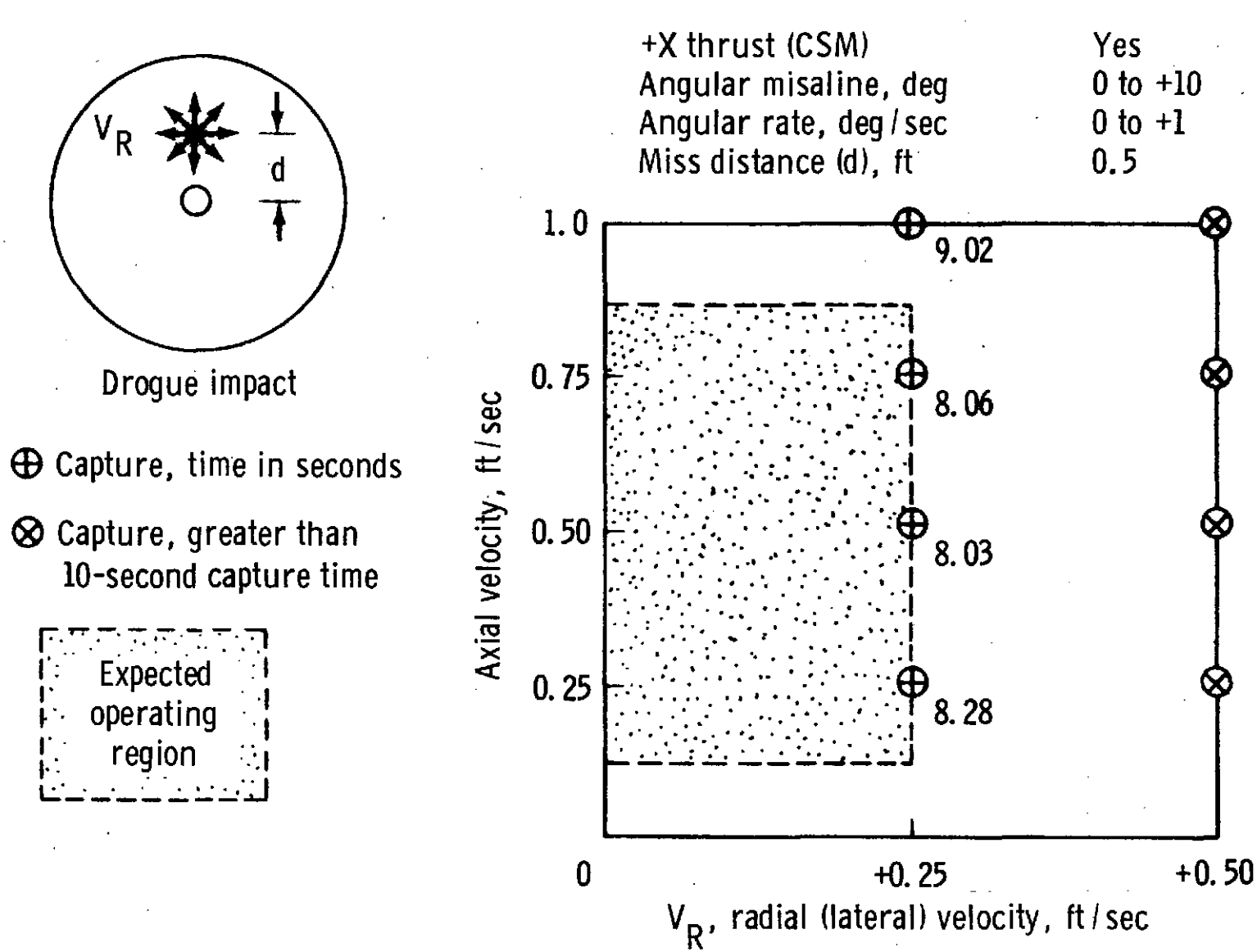

Figure 10.- Mission G, LOD capture boundaries for axial versus radial velocity with CSM thrust.

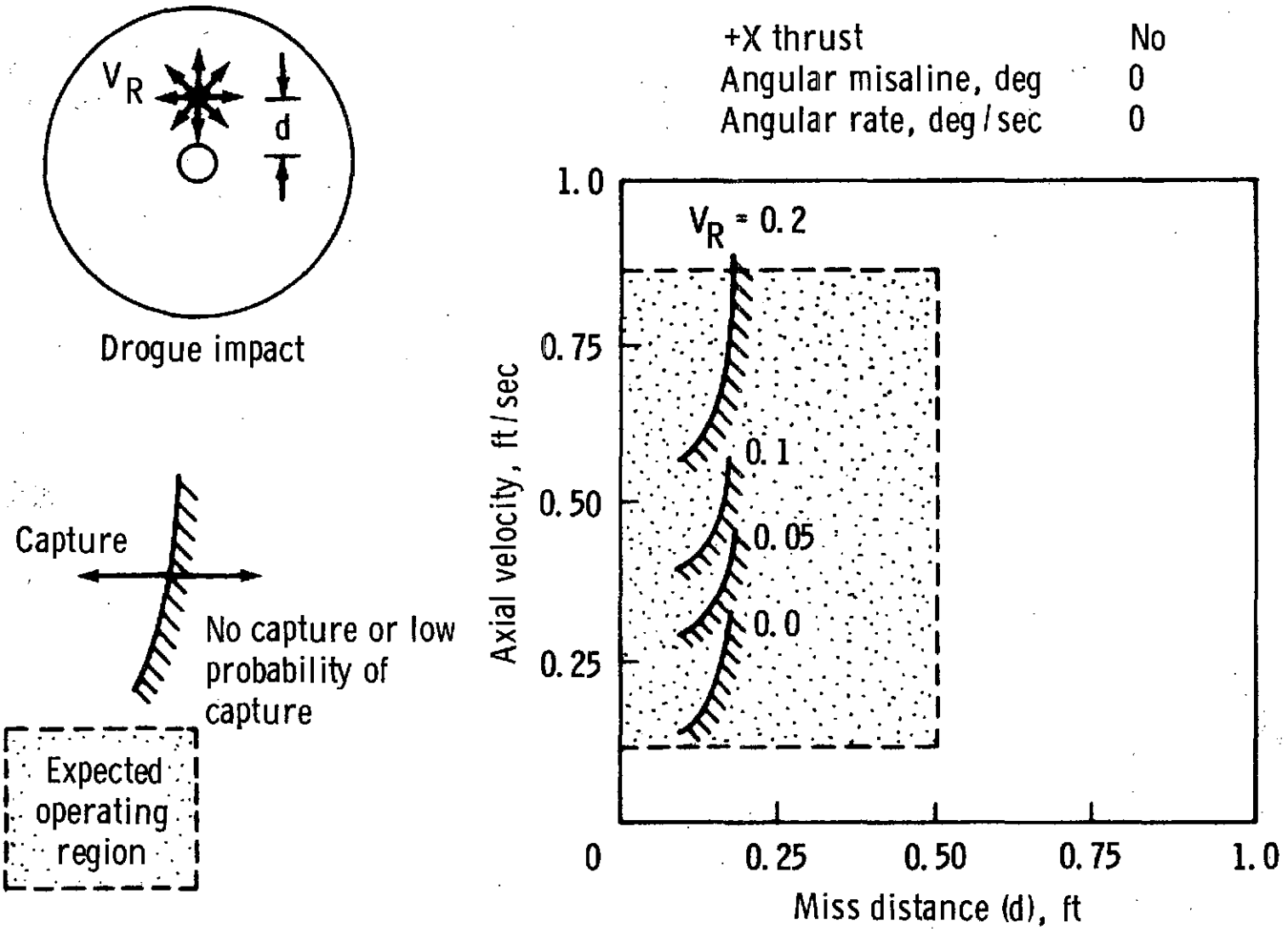

Figure 11.- Mission D, LOD capture boundaries for axial velocity versus radial miss distance with no thrust.

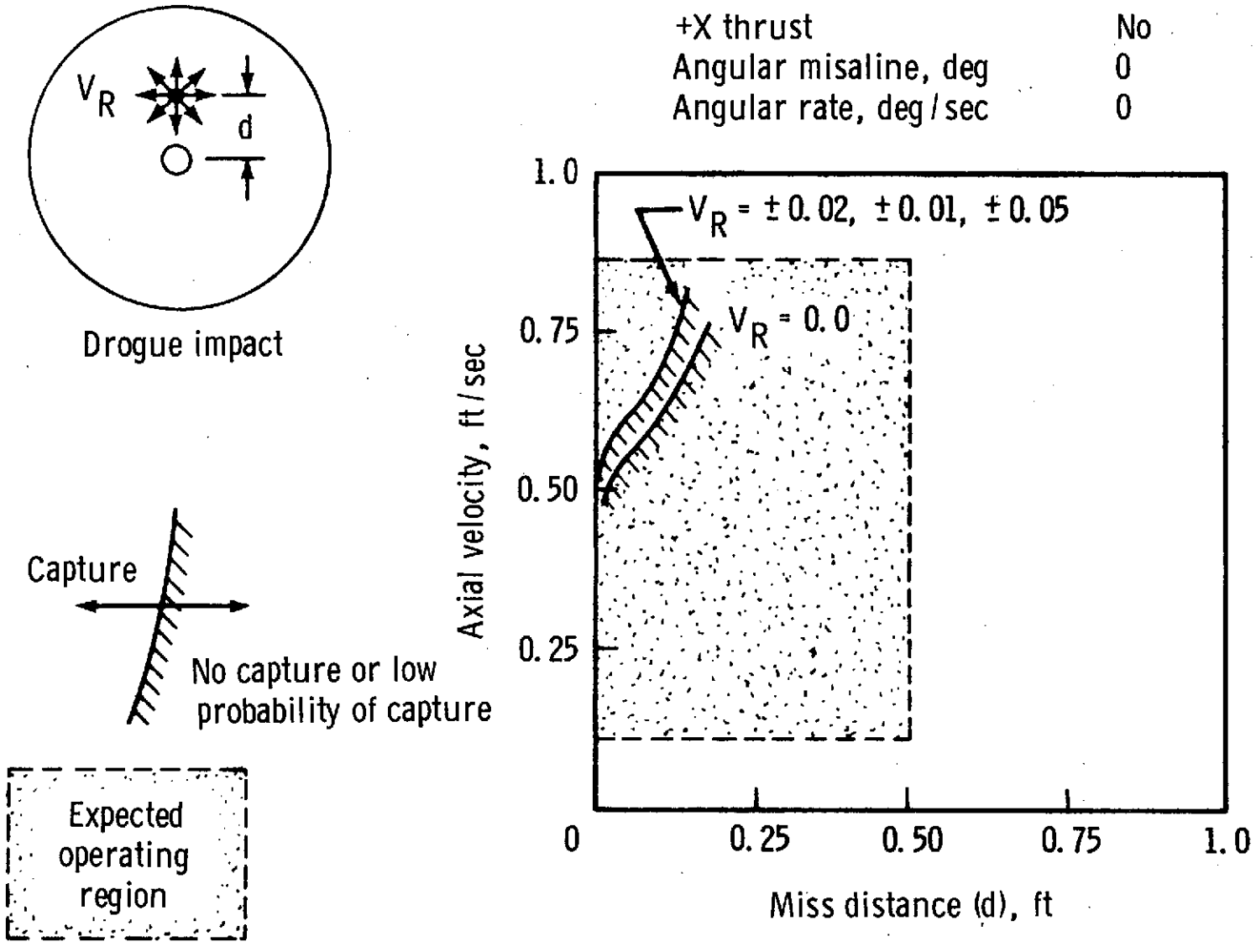

Figure 12.- Mission G, LOD capture boundaries for axial velocity versus radial miss distance with no thrust.